Evaluations of Thin Cirrus Contamination and Screening in Ground Aerosol Observations Using Collocated Lidar Systems

Jingfeng Huang[1,2], N. Christina Hsu[2], Si-Chee Tsay[2], Brent N. Holben[2], Ellsworth J. Welton[2], Alexander Smirnov[2,5], Myeong-Jae Jeong[3], Richard A. Hansell[2,4], Timothy A. Berkoff [2,6]

[1] **Morgan State University, Baltimore, Maryland, USA.**
[2] **NASA Goddard Space Flight Center, Greenbelt, Maryland, USA.**
[3] **Gangneung-Wonju National University, Gangneung, Gangwon-do, Korea.**
[4] **University of Maryland College Park, College Park, Maryland, USA.**
[5] **Sigma Space Corporation, Lanham, Maryland, USA.**
[6] **University of Maryland Baltimore County, Baltimore, Maryland, USA.**

***Contact:** jingfeng.huang@nasa.gov

Popular Summary

Satellite data play irreplaceable roles in large-scale aerosol observations and relevant global climate change studies. However the accuracy of satellite aerosol retrievals heavily relies on ground measurements because ground-based aerosol observations play an important role in calibrating and validating their spaceborne counterparts. Uncertainties associated with satellite data retrieval algorithms are still at large not well quantified. Cirrus clouds, particularly sub visual high thin cirrus with low optical thickness, are difficult to be screened in operational aerosol retrieval algorithms.

Collocated aerosol and cirrus observations from ground measurements, such as the Aerosol Robotic Network (AERONET) and the Micro-Pulse Lidar Network (MPLNET), provide us with an unprecedented opportunity to examine the susceptibility of operational aerosol products to thin cirrus contamination. Quality assured aerosol optical thickness (AOT) measurements were also tested against the CALIPSO vertical feature mask (VFM) and the MODIS-derived thin cirrus screening parameters for the purpose of evaluating thin cirrus contamination.

Key results of this study include: (1) Quantitative evaluations of data uncertainties in AERONET AOT retrievals are conducted. Although AERONET cirrus screening schemes are successful in removing most cirrus contamination, strong residuals displaying strong spatial and seasonal variability still exist, particularly over thin cirrus prevalent regions during cirrus peak seasons, (2) Challenges in matching up different data for analysis are highlighted and corresponding solutions proposed, and (3) Estimation of the relative contributions from cirrus contamination to aerosol retrievals are discussed.

Such evaluation and examination are valuable for improving operational ground aerosol retrieval algorithms in related to cirrus screening and potential cirrus contamination correction. The results are valuable for better understanding and further improving ground aerosol measurements that are critical for aerosol-related climate research.

Evaluations of Thin Cirrus Contamination and Screening in Ground Aerosol Observations Using Collocated Lidar Systems

Jingfeng Huang[1,2], N. Christina Hsu[2], Si-Chee Tsay[2], Brent N. Holben[2], Ellsworth J. Welton[2], Alexander Smirnov[2,5], Myeong-Jae Jeong[3], Richard A. Hansell[2,4], Timothy A. Berkoff [2,6]

[1] Morgan State University, Baltimore, Maryland, USA.

[2] NASA Goddard Space Flight Center, Greenbelt, Maryland, USA.

[3] Gangneung-Wonju National University, Gangneung, Gangwon-do, Korea.

[4] University of Maryland College Park, College Park, Maryland, USA.

[5] Sigma Space Corporation, Lanham, Maryland, USA.

[6] University of Maryland Baltimore County, Baltimore, Maryland, USA.

***Contact:** jingfeng.huang@nasa.gov

Abstract:

Cirrus clouds, particularly sub visual high thin cirrus with low optical thickness, are difficult to be screened in operational aerosol retrieval algorithms. Collocated aerosol and cirrus observations from ground measurements, such as the Aerosol Robotic Network (AERONET) and the Micro-Pulse Lidar Network (MPLNET), provide us with an unprecedented opportunity to examine the susceptibility of operational aerosol products to thin cirrus contamination. Quality assured aerosol optical thickness (AOT) measurements were also tested against the CALIPSO vertical feature mask (VFM) and the MODIS-derived thin cirrus screening parameters for the purpose of evaluating thin cirrus contamination. Key results of this study include: (1) Quantitative evaluations of data uncertainties in AERONET AOT retrievals are conducted. Although AERONET cirrus screening schemes are successful in removing most cirrus contamination, strong residuals displaying strong spatial and seasonal variability still exist, particularly over thin cirrus prevalent regions during cirrus peak seasons, (2) Challenges in matching up different data for analysis are highlighted and corresponding solutions proposed, and (3) Estimation of the relative contributions from cirrus contamination to aerosol retrievals are discussed. The results are valuable for better understanding and further improving ground aerosol measurements that are critical for aerosol-related climate research.

1. Introduction

Satellite data play irreplaceable roles in large-scale aerosol observations and relevant global climate change studies (e.g. Andreae, 1991; Breon et al, 2002; Menon et al, 2002; Huang et al., 2009). However the accuracy of satellite aerosol retrievals heavily relies on ground measurements because ground-based aerosol observations play an important role in calibrating and validating their spaceborne counterparts (Holben et al., 1998). Uncertainties associated with satellite data retrieval algorithms are still at large not well quantified (e.g. Myhre et al. 2005); cloud screening and quality control in ground data retrievals are also challenging (Smirnov et al., 2000; Schaap et al., 2009). For example, the existence of high thin cirrus clouds with low optical thickness, are still sometimes observed in the satellite and ground aerosol products (e.g. Gao et al, 2002a; Kaufman et al., 2005; Huang et al., 2011). Therefore, it is imperative to perform rigorous and systematic global evaluations on the severity of cirrus contamination in ground aerosol products and to investigate better alternatives for cirrus screening schemes.

With concurrent cirrus observations from ground or spaceborne lidars, quantitative evaluation of thin cirrus contamination in the operational aerosol products becomes possible (e.g. Huang et al., 2011). For ground observations, aerosol retrievals from the Aerosol Robotic Network (AERONET, Holben et al., 1998) and atmosphere profiling from the Micro-Pulse Lidar Network (MPLNET, Welton et al., 2001) provide simultaneous measurements at their collocated sites. For satellite observations, with the advent of the A-Train satellite constellation, global cirrus cloud coverage and its temporal and spatial variability can be comprehensively observed for the first time (Sassen and Liu, 2008; Massie et al, 2010). The collocated MODIS-derived thin cirrus parameters and cloud-aerosol lidar and infrared pathfinder satellite observations (CALIPSO) provide us with an unprecedented opportunity to examine the susceptibility of the ground aerosol products to cirrus contamination and to evaluate the robustness of current cirrus screening techniques. Such evaluation and examination are valuable for improving operational ground aerosol retrieval algorithms in related to cirrus screening and potential cirrus contamination correction.

For the current AERONET aerosol optical depth (AOT) cloud screening, a series of procedures are adopted by examining the temporal variability of measured AOT (Smirnov et al., 2000). AERONET cloud screening based on temporal variability is effective for eliminating most cloud contamination (e.g., Smirnov et al., 2000; Kaufman et al., 2006); however, residual cirrus contamination in the operational aerosol products are still observed (e.g., Gao et al, 2002a; Kaufman et al., 2005; Schaap et al., 2009; Huang et al., 2011), that warrant in-depth investigations in this study by taking advantage of ground and spaceborne lidar observations for detecting cirrus.

For those collocated AERONET and MPLNET sites, lidar measurements from MPLNET can provide observational evidence of thin cirrus to help verify the susceptibility of aerosol data to thin cirrus contamination. Similarly, spaceborne lidar observations from CALIPSO can provide an alternative cirrus observation reference, if the CALIPSO tracks are not far from the AERONET sites. Additionally because cirrus clouds usually occur at higher altitude (> 10 km in the tropical region) and are commonly associated with ice clouds, detecting cirrus from satellites, such as MODIS, is based on apparent reflectance at 1.38 μm, 0.66 μm, and 1.24 μm, and brightness temperature differences in the thermal bands (e.g., Gao and Kaufman, 1995; Gao et al. 2002a, 2002b; Roskovensky and Liou, 2003; Roskovensky et al., 2004). In order to scale the effect of water vapor absorption, reflectance at a second channel is usually required in the practical algorithms (Gao et al., 2002b). A ratio between the MODIS apparent reflectance at bands 1.38 μm and 0.66 μm was preferred over other satellite-derived cirrus screening parameters for detecting cirrus over Southeast Asia during the cirrus prevailing season (Huang et al., 2011).

Therefore, as an extension of a detailed regional study in the Biomass-burning Aerosols in South East-Asia: Smoke Impact Assessment (BASE-ASIA) campaign (Huang et al., 2011), this study aims to:

- Investigate the consistency and comparability of detecting cirrus using MPLNET and CALIPSO
- Investigate the susceptibility of ground aerosol measurements to cirrus contamination and to quantify its influence at additional AERONET sites. This goal is achieved by exploring the susceptibility of valid and quality assured aerosol retrievals to identifying thin cirrus in the following pairs of matched up data: AERONET vs. MPLNET; AERONET vs. CALIPSO, and AERONET vs. MODIS
- Evaluate the relative contributions of cirrus optical depth to aerosol observations for those cirrus contaminated cases and to examine the corresponding changes in the Ångström exponent

- Discuss various factors that impact the data match up schemes used in this study and to recommend solutions for future studies.

This paper is arranged as follows. Section 2 lists the main datasets used in this study, followed by a detailed demonstration of results given in Section 3. Lastly, section 4 presents our main findings and conclusions.

2. Data and Data Processing

Because the main focus of the study is on ground measurements, the primary datasets for this study are concurrent ground aerosol and cirrus observations, complemented by cirrus observations from satellites. For aerosol retrievals, we used aerosol products from AERONET; for cirrus identification, we employed data from MPLNET, CALIPSO vertical feature mask (VFM) and the MODIS-derived thin cirrus parameter.

2.1. AERONET

The AERONET provides a long-term, continuous and readily accessible public domain database of aerosol optical, microphysical and radiative properties for aerosol research and characterization, validation of satellite retrievals, and synergism with other databases (Holben et al., 1998). For the current AERONET aerosol optical depth (AOT) cloud screening, a series of procedures are adopted by examining the temporal variability of measured AOT (Smirnov et al., 2000), including the AOT variability from three consecutive measurements (triplet) over a one-minute time interval, the standard deviation of the remaining AOT (500 nm) data points over a day, and observations of AOT (500 nm) and Ångström exponent with variability higher than three standard deviations within the daily intervals.

For this study, only cloud-screened and quality-assured Level 2.0 data were used for the highest operational quality. An AOT temporal variability based three-step approach is adopted in the current operational cloud screening (Smirnov et al., 2000). We use the level 2.0 AOT measurements at 440 nm to validate against concurrent cirrus observations for computing susceptibility statistics.

2.2. MPLNET

The collocated MPLNET and AERONET super sites provide both column and vertically resolved aerosol and cloud data, such as: optical depth, single scatter albedo, size distribution, aerosol and cloud heights, planetary boundary layer (PBL) structure and evolution, and profiles of extinction and backscatter (Welton et al., 2001; http://mplnet.gsfc.nasa.gov). Out of 16 collocated MPLNET and AERONET sites, 13 sites with overlapping temporal data coverage were selected. We primarily use MPLNET Level 1.0 normalized relative backscatter (L1.0 NRB) data for cirrus visualization and cirrus flag derivation. The NRB-derived cirrus flag is used for automated cirrus identification purposes. It is generated based on the statistical characterization of the NRB data in each time-space window (300-m in range and 10-minute in time). To be discriminated from a more theoretical based cirrus flag, this cirrus flag is named as 'Statistical Cirrus Flag' (SCF) in this paper. Although MPLNET has both day and night observations and noise level generally increases in daytime, we had to use daytime data because AERONET data are daytime measurements. The following criteria were applied in each time-space window of the NRB data to identify the existence of cirrus cloud and to minimize the influence from noise: 1) the total number of samples has to exceed 30; 2) the averaged NRB value has to exceed 0.35 and 3) cloud base height has to be higher than 8 km. The selection of the threshold values were based on visual inspections of many cases by comparing the cirrus flag to the NRB profiles to ensure the cirrus features were separated from surrounding noise and from the aerosol and low cloud layers underneath. It is noteworthy, however, that for the Monterey and Trinidad-Head sites, the trans-pacific aerosol layers can be as high as cirrus base heights (e.g. Eguchi et al., 2009). In such circumstances, we increased the cirrus cloud base height of the NRB-derived cirrus flag to 10 km to avoid misidentifying aerosol layers at high altitude as cirrus. Although this conservative solution may underestimate the occurring frequency of cirrus clouds, it gives us more confidence on cirrus detection.

Moreover, once SCF identifies cirrus during a 10-minute window, a cirrus persistence flag (CPF) is designed to count the continuity of NRB samples that have NRB values exceeding 0.35 at each 1-minute MPL sampling step within the 10-minute time window. The threshold value was determined based on its effectiveness to distinguish cirrus features from ambient noise. CPF will be used to test the persistence of cirrus during each 10-minute window. The effectiveness of SCF and CPF in cirrus detection will be elaborated in Section 3.

Cirrus case identification highly depends on selection criteria. Based on the SCF and

CPF, we will test four sets of cirrus selection criteria based on cirrus existence and persistence within different time window (TW): 'TW10 existence', 'TW30 existence', 'TW30 overall persistence' and 'TW30 strong persistence', from less strict to most strict, respectively.

1) 'TW10 existence' uses SCF at each 10-minute time window without any additional cirrus persistence testing;
2) 'TW30 existence' uses SCF at three consecutive 10-minute time windows, without any additional cirrus persistence testing;
3) 'TW30 overall persistence' uses both SCF and CPF at three consecutive 10-minute time windows and requires CPF values higher than 20 out of 30 samples at each one-minute MPL sampling resolution within the 30-minute time window;
4) 'TW30 strong persistence' is the strictest, and it uses both SCF and CPF at three consecutive 10-minute time windows and requires CPF values higher than 9 out of the 10 samples within each 10-minute time window, and such requirements have to be met for all three consecutive windows. The difference in the results of these four settings will be discussed when they are used for the AERONET-MPLNET match up in Section 3.3.

2.3. CALIPSO

CALIPSO combines an active lidar instrument (CALIOP) with passive infrared and visible imagers to probe the vertical structure and properties of clouds and aerosols over the globe (Vaughan et al., 2005, 2009). It provides a unique capability to closely examine the vertical profiles of aerosol and clouds from space. For this study, the Level 3.0 CALIPSO vertical feature mask (VFM) v3.01, that includes a 'transparent thin cirrus' cloud subtype (Vaughan et al., 2005, 2009; Liu et al., 2009), were used as baseline for cirrus cloud detection. For comparison to concurrent AERONET aerosol measurements in terms of cirrus contamination evaluation, only daytime CALIPSO data were used. For comparison to MPLNET in terms of cirrus detection, both daytime and nighttime CALIPSO data were used.

2.4. MODIS

For this study, only Aqua MODIS data were used to identify thin cirrus.. The primary datasets for cirrus screening are the MYD021KM level 1B collection 5 data that has apparent reflectance at 1.38 μm (R1.38) and its derived reflectance ratio between bands 1.38 μm and 0.66 μm (RR1.38/0.66) to be used as indicators for thin cirrus at relatively large scale (Huang et al., 2011).

3. Results

3.1 Thin Cirrus Climatology from CALIPSO

Thin cirrus climatology and its seasonal and regional variability are crucial to understanding their links to data uncertainties in aerosol products. In this study, thin cirrus occurrence frequency is calculated solely based on CALIPSO VFM. The following three criteria were set accordingly to ensure the classification of cirrus clouds is appropriate:

1) The confidence level for the feature type in VFM has to exceed 70 in the cloud-aerosol discrimination (CAD) score, which signifies high confidence on cloud rather than aerosol;

2) The feature type should be ‘cloud’, and the sub feature type should be ‘cirrus clouds transparent’; and

3) Surface return signal should be detected. This is because if the lidar signal is totally attenuated and there is no surface return detected, clouds are too thick (optical thickness higher than 3.0) to be classified as thin cirrus (Sassen et al. 2008).

Based on these criteria, we calculated daytime thin cirrus occurrence frequency as shown in Figure 1. Only daytime statistics were shown because aerosol retrievals are only available at daytime. A global average of 18% in Figure 1(a) is comparable to 15% in Sassen et al. (2008) where they also constrained cloud top temperature to be less than -40°C from CloudSat data in order to distinguish pure ice clouds from mixed phase clouds. Cirrus average height and its latitudinal dependence in Figure 1(b) are also similar to Sassen et al. (2008). While the global distribution of cirrus occurrence is highly consistent to Sassen et al (2008), it is noteworthy that the Tibet Plateau features much higher thin cirrus occurrence frequency than that in Sassen et al. (2008), which might be attributable to their additional control of cloud top temperature. The seasonal migrations of thin cirrus prevailing regimes are also clearly seen in the thin cirrus occurrence frequencies in four seasons.

3.2. MPLNET versus CALIPSO

Before comparing concurrent aerosol and cirrus observations, it is intriguing to compare the cirrus detection capability of ground lidar and its spacebore counterpart, by crosschecking the effectiveness of MPLNET NRB-derived cirrus flag and the CALIPSO vertical feature mask. A quantitative direct comparison between MPLNET and CALIPSO may be challenging (Berkoff et al., 2008) however an indicative qualitative comparison in terms of cirrus existence is feasible. The most challenging issue remains to be the distance between the MPLNET sites and CALIPSO overpass tracks. Another challenge is that, in some cases, the CALIPSO overpass time is close to the MPL shutdown time when the MPL was turned off around solar noon to avoid strong sunlight from entering the telescope, which is more critical for tropical sites that have very small solar zenith angle around high noon (Welton, personal communication). Additionally the CALIPSO 16-day repeat cycle also significantly reduces the sample size of MPLNET-CALIPSO collocation.

A first-step crosscheck between MPL and CALIPSO is the cirrus occurrence seasonality. We selected four AERONET-MPLNET sites (GSFC, COVE, Trinidad_Head and NCU_Taiwan) that exhibit the longest multiple year data coverage to give equal sampling weight to different seasons. Table 1 tabulated the cirrus occurrence seasonality as observed from both MPLNET and CALIPSO. For MPLNET data, we calculated cirrus occurrence frequency as a percentage of MPLNET detected cirrus cases at each 10-minute time window over the total number of MPLNET 10-minute time windows during the one-hour period +/- 30 minutes around the averaged CALIPSO local overpass time (around 13-14 local hour). The values for CALIPSO are thin cirrus occurrence frequency observed from all CALIPSO tracks that overpass and are within the 1°×1° degree grid centered at each site. The frequencies for all four seasons were calculated with the annual mean shown in Figure 1. For each season and annual mean, the thin cirrus occurrence frequency values at the closest grid to the site were used in Table 1.

Overall, the annual mean of cirrus frequency from MPLNET and CALIPSO are comparable in their order of magnitudes: 14.10 vs. 18.56, 12.62 vs. 16.56, 8.13 vs. 16.12, 5.36 vs. 8.66 percent for GSFC, COVE, Trinidad_Head and NCU_Taiwan, respectively. For all four sites, the MPLNET and CALIPSO agreed on the thin cirrus peak seasons: GSFC, COVE and NCU for JJA, and Trinidad_Head for MAM. Three out of the four sites agreed on the least cirrus occurrence frequency (COVE for SON, Trinidad_Head for JJA, and NCU for DJF) except GSFC where MPLNET exhibited a low cirrus season for MAM but for CALIPSO the low cirrus season was SON. Although they both agree on the cirrus peaks seasons, the discrepancy is also significant: the CALIPSO detected cirrus frequencies for the peak seasons were generally higher than those for the MPL: 20.30% vs. 15.65%, 24.33% vs. 13.95%, 32.65% vs. 12.27%, and 17.66% vs. 9.59% for GSFC, COVE, Trinidad_Head and NCU sites, respectively. There are two possible reasons for such discrepancies: First, the CALIPSO's 'top-down' viewing geometry allows better detection of high clouds before the lidar signal become attenuated; However, in the MPL's 'bottom-up' viewing geometry, lidar signals could be attenuated by aerosol layers and low clouds significantly before it reaches high clouds. Secondly, noontime measurements are always difficult for ground lidar, because the noise levels are usually much higher when the solar zenith angle is low which makes automated cirrus detection more challenging. Moreover the MPL lidar noontime shout-down protective measure also prevents continuous observations of thin cirrus around local noontime. This second factor is expected to have a bigger impact on tropical sites during boreal summer time, such as NCU_Taiwan with a 17.66% vs. 9.59% difference.

To gain more insight on the comparability between MPLNET and CALIPSO, we further matched up 9 MPLNET-AERONET collocated sites (See Table 2). To ensure a one-to-one match up of the data, we only chose those data pairs with the closest distance of CALIPSO track to the site and the closest MPLNET data collection time (within ±5 minutes) to the CALIPSO overpass. Because CALIPSO overpass tracks shift slightly within a range of ~15-20 km between tracks during the 16-day repeat cycle at each site, the distance between the sites and CALIPSO tracks also varies in range. Seen from Table 2, among the 9 sites, some sites (i.e. Gosan_SNU) have a distance range less than 10 km, but other sites (i.e. GSFC) can have larger ranges up to 90 km. Despite all the challenges and the limited sample size of collocated cases, close examination of all cirrus cases from June 2006 to December 2010 indicated that, in terms of cirrus detection, for the 8 sites (except Singapore) that have more than 20 matchups (~ one year of day or night data coverage considering 16-day CALIPSO data cycle), MPLNET and CALIPSO reached a percentage agreement of 71-88% when both daytime and nighttime cases were counted. The agreement results are not much different between daytime and nighttime. This not only proves the general comparability of the MPLNET L1.0 SCF and the CALIPSO VFM in terms of cirrus detection, but it also demonstrates the effectiveness of MPL L1.0

SCF for detecting cirrus without significant impacts from large noise during the daytime. A very noteworthy point is that when MPLNET cirrus criteria were set much tighter, for example, from “TW10 existence” to “TW30 strong persistence”, the number of cirrus cases decreased significantly. Such sensitivity to cirrus detection criteria impacts the AERONET-MPLNET match up significantly, which contributes to the discrepancy between the results from the AERONET-MPLNET match up and the results from the AERONET-CALIPSO match up, in addition to the already existing temporal and spatial differences of matched up samples. This sensitivity will be further discussed in the following sections.

3.3. AERONET versus MPLNET

3.3.1. AERONET-MPLNET Match up

The AERONET Aerosol optical thickness (AOT) retrievals were paired up with the MPLNET NRB-derived SCF and CPF to calculate susceptibility percentage (%, SP), an indicator of how many percentages of best quality assured L2.0 AOT retrievals are potentially contaminated by cirrus. Results about SP will be discussed in Section 3.3.2. The MPLNET SCF and CPF calculations and the four MPLNET cirrus detection criteria settings were discussed in Section 2.2. Additional requirements for the one-to-one AERONET-MPLNET match up are:

1) At each of the four MPL cirrus settings, AERONET has to have valid quality assured L2.0 AOT retrievals at 440 nm within the central MPL SCF 10-minute time window, to be counted as being potentially susceptible to cirrus contamination;

2) At each match up, the solar zenith angle (SZA) has to be less than 20°. This is because the micro-pulse lidar is looking upright through the atmosphere for aerosol-cloud features while sunphotometer is always looking at the sun for AOT retrievals. The less the solar zenith angle, the atmospheric paths as observed by both instruments are better matched up. They never exactly overlap however, because the micro-pulse lidar cannot look into the sun.

To further elaborate on the AERONET-MPLNET match up, Figure 2 shows the MPL NRB, SCF, and CPF in their respective (a)-(c) panels for the cirrus case over the COVE site on June 7, 2007. The persistent cirrus layer around 11-12 km altitude was clearly seen from the NRB profile (Figure 2a). After statistical analysis, both SCF and CPF showed their consistent results with the NRB observations. SCF in Figure 2(b) shows the corresponding NRB values when cirrus existence was identified at each 10-minute time window. In comparison to Figure 2(a), Figure 2(b) shows that the SCF filtering process removed most of ambient noise effectively, demonstrating that SCF is capable of distinguishing cirrus layers from noise very effectively. CPF in Figure 2(c) on the other hand described the continuity of the cirrus layers that had persistent strong lidar scattering signals (NRB>0.35). Therefore when low cloud attenuated the lidar signals significantly, for example the case around 10:40AM, the CPF number decreased correspondingly because of the weaker NRB strength. The corresponding AERONET measurements, including AOT (440 nm), AOT (500 nm), Ångström exponent (440-675 nm) susceptible to cirrus contamination, and solar zenith angle, are also shown in Figure 2(d). It is noteworthy however that the aerosol measurements around 9AM local hour were not counted as cirrus contaminated cases because SZA was 41°, which did not pass the SZA<20º test.

3.3.2. Susceptibility Percentage (SP)

Susceptibility percentage (SP) is defined as the percentage of aerosol retrievals that are susceptible to cirrus contamination to the total numbers of quality aerosol retrievals. Because match up criteria can be less strict or very strict, SP values change with different settings of match up criteria. Table 3 summarizes the sensitivity of SP to cirrus existence and persistence criteria settings, time window selections, and SZA, for all 13 sites with their temporal coverage sorted in order. As seen in Table 1, changes in SP can be an order of magnitude simply because of different cirrus selection criteria. For example, the SP values at GSFC were 7.74%, 3.61%, 3.44% and 1.55% for 'TW10 existence', 'TW30 existence', 'TW30 overall persistence' and 'TW30 strong persistence' respectively. The reasons are twofold: one is the actual spatial and temporal variability of cirrus clouds, the other is the way that lidar looks upright for high cloud detection and gets attenuated along the atmospheric path. Although cirrus usually occur at synoptic scales, low clouds, aerosol and the atmosphere can significantly attenuate the MPL lidar signal, before it reaches more than the 10 km height to detect cirrus. Therefore any occurrence of heavy low or middle cloud or heavy aerosol could prevent continuous observation of cirrus. Note that this impact gets particularly stronger around noontime when noise levels usually increase significantly (See Figure 2(a)), which makes cirrus detection even more challenging as it requires relatively stronger lidar signals in order to discriminate cirrus from ambient noises. Moreover, the MPL lidar shutdown around high noon at low SZA hours also prevented continuous observations of cirrus persistence, particularly for tropical sites. Thus additional strong persistence testing (e.g., 'TW20 strong persistence') resulted in much lower SP values than relatively weaker persistence testing (e.g., 'TW10 existence'). SP values for the top 10 AERONET-MPLNET sites from the 'TW30 overall persistence' testing are plotted on top of the CALIPSO thin cirrus occurrence frequency map in Figure 3. With the 'TW30 overall persistence' testing and the SZA filtering (SZA<20º), all 10 sites have SP values less than 5% and 4 of them (40%) are actually less than 1% (Figure 3); but for the 'TW10 existence' testing, 6 out of 10 sites (60%) have SP values within 4-10%, and the other 4 (40%) within 1-3%. Similarly in Table 3, when the time window becomes larger, for example, changing cirrus detection from 15-minute time window to 30-minute or 60-minute time windows, the requirements for cirrus strong persistence also become higher, thus less cirrus cases were detected, and SP values become lower correspondingly. For example, at GSFC, the SP values for TW15, TW30 and TW60 were 3.10%, 1.55% and 1.20% respectively.

Viewing geometry differences between the sunphotometer and micro-pulse lidar can affect the SP assessment dramatically. For example for GSFC, the SP value increases significantly from 1.55% to 3.29% when the SZA constraint changes from SZA<20º to all SZA applying the 'TW30 strong persistence' test (See Table 3). The 'SZA<20º' control is conducted to account for the viewing geometry differences between sunphotometers and lidar instruments. A 'SZA<20º' criterion ensures a better matchup. On the downside however, a 'SZA<20º' screening significantly reduced the sample sizes. For comparison, 'all SZA' match ups had many more cirrus cases detected than

‘SZA<20º’. For example, the number of cirrus cases for ‘TW60’ at GSFC (Table 2) was found to be 730 versus 7.. However, it is worthwhile to emphasis that the AERONET-MPLNET match ups that sample at higher SZA (i.e. SZA > 20) are less indicative of cirrus contamination in the AERONET measurements because the two instruments were more likely looking at different atmospheric paths when their viewing angles were widely separated.

Seasonal variability was also found in the SP statistics. The derived SP values shown in Figure 3 and tabulated in Table 3 features strong seasonal signals. Table 4 compares cirrus statistics of SP values and samples for their seasonality over the 13 sites. For example, cirrus cases occurred more frequently in boreal spring for Pimai and in boreal summer for GSFC and COVE (also see Table 1). All the 10 cirrus cases in the ‘TW30 strong persistence’ testing over GSFC were from boreal summer. Both ‘TW10 existence’ and ‘TW30 overall persistence’ tests indicate similar seasonality of cirrus occurrence at each site.

3.3.3. Cirrus Optical Depth Calculation for Selective Cases

We further investigated each individual cirrus case identified in the AERONET-MPLNET match up for more details. With given NRB and molecular backscatter profiles, molecular optical depth can be calculated from molecular extinction profiles based on NCEP vertical temperature and pressure profiles, thus theoretically cirrus optical depth can also be calculated:

$$P_1=C\times\beta_{m1}\times e^{[-2(\tau_{m1}+\tau_{c1})]} \quad (1)$$

$$P_2=C\times\beta_{m2}\times e^{[-2(\tau_{m2}+\tau_{c2})]} \quad (2)$$

Where subscripts 1 and 2 denote cirrus base and top, respectively. P, β and τ are NRB, molecular backscatter and optical depth respectively, while m and c stand for molecular and cirrus. C is a coefficient that counts for lidar performance and lidar signal attenuation due to other aerosol or cloud layers beneath cirrus. All these parameters are retrieved at cirrus base and cirrus top heights. From (1) and (2), cirrus optical depth can be calculated as:

$$\Delta\tau_c = \tau_{c2} - \tau_{c1}=0.5\times[\ln(P1/P2)-\ln(\beta_{m1}/\beta_{m2})]-(\tau_{m2}-\tau_{m1}) \quad (3)$$

The challenge however comes from the following two influential factors that prevent precise measuring of NRB values at high altitude in daytime: 1) Ground lidar signal becomes extremely weak when it reaches an altitude higher than 10 km where cirrus layers reside, particularly after being further attenuated by cirrus; 2) during daytime, particularly around local noon time when the AERONET-MPLNET match up requires the closeness of viewing geometries from both instruments (SZA<20º), noise level also increases significantly (see Figure 2(a)). Therefore operational cirrus optical depth estimation based on the MPL dataset faces extreme difficulties. In this work, we selected a very limited numbers of quality cirrus cases for testing an empirical approach for calculating cirrus optical depth, in the scope of evaluating relative contribution of cirrus optical depth to total optical depth observed by the sunphotometer. We assessed all cases for lidar operational stability, lidar signal strengths before and after cirrus layers, and persistence of cirrus layers. Results from two test cases over the GSFC site on June 7th 2007 are shown in Figure 4.

Figure 4(a) shows a very persistent cirrus layer lasting for more than 8 hours over GSFC on June 7th 2007. To overcome the influence from noise, we used the data distribution pattern from the concurrent molecular backscatter profile to proxy the NRB data distributions beneath and above cirrus layers (Figure 4(b) and (c)). The assumption is that in the clear portions of the atmosphere (i.e. above aerosol and low clouds but below cirrus clouds), the data distribution pattern of the NRB profile is similar to the data distribution pattern of the molecular backscatter profile. Such data similarity, indicating molecular scattering profiles without cloud and noise interference, has been broadly discussed in previous literatures (e.g. Sassen et al., 1989; Vaughan et al., 2005, 2009). This assumption was further verified from MPLNET night scene observations when noise levels were significantly low. For these two particular cases, the measured NRB profile data from 4 km to 10 km and the collocated molecular backscatter profile data were trained to find a best linear fit function between the two datasets. This best fit function was then applied to the molecular backscatter data to approximately calculate the NRB data right beneath and just after cirrus layers. Then, cirrus optical depth can be calculated in equation (3) by using the approximated NRB values, the molecular backscatter and molecular optical depth data as inputs. The molecular backscatter and optical depth were calculated from a Rayleigh radiative model based on inputted NCEP reanalysis temperature and pressure profiles. Results show roughly 30-50% relative contributions from cirrus to the possibly ‘cirrus-contaminated’ AOT retrievals at 527 nm, 0.0926 vs. 0.270 for 16:12UTC case, and 0.123 vs. 0.253 for the 16:22UTC case. However, despite the residual profile-fitting uncertainties, this level of cirrus optical depth did not seem to decrease Ångström exponent significantly to a very low value, while the Ångström exponents were still as high as 1.0 for both cases even under cirrus contaminations.

3.4. AERONET versus CALIPSO

Another approach for assessing cirrus contamination in the AERONET AOT retrievals is to pair them up with CALIPSO cirrus observations. The complication, however, comes from the limited CALIPSO temporal coverage at each site because of the 16-day repeating cycle and the distant between the CALIPSO overpass tracks and most AERONET sites. To address these issues, we first sorted the distances between the locations of 522 AERONET sites that have L2.0 AOT retrievals and the CALIPSO's 16-day cycle of global overpass tracks during the first 16 days of 2010 (January 1-16, 2010). Then we selected the top 56 sites whose distances to CALIPSO tracks are within 30 km. At these 56 sites, we collocated CALIPSO cirrus flags with AERONET L2.0 AOT retrievals. Because CALIPSO tracks fluctuate from one 16-day global track to another, actual distances from these AERONET sites to the CALIPSO tracks were calculated for each match up data pair. We further constrain the calculated (actual) distance to be less than 10 km. Moreover, the one-to-one data match up was further constrained by limiting the CALIPSO overpass time to be within +/-10 minutes of the AERONET data collection time. To ensure sufficient statistical reliability, the total sample size of matched-up data has to exceed 20 for each AERONET site, roughly corresponding to about one-year of CALIPSO and AERONET paired data, considering CALIPSO's 16-day cycle. After matching up the data, the resulting SP values for the 18 AERONET sites that passed time and space filtering are presented in Figure 5, superimposed on an annual mean thin cirrus occurrence frequency map. About half (8 out of 18) sites have SP values less than 10%, which means there is a relative low level of susceptibility of AOT retrieval to thin cirrus contamination (Figure 5(a)). This level of SP values is relatively comparable in the order of magnitude to the AERONET-MPLNET 'TW10 Existence' testing (See Table 3). However, some sites showed much larger SP values, for example, 33% for CARTEL, 23% for CEILAP-BA, and 21% for Xianghe that are outside of the cirrus prevailing regions, and 25% for Ilorin which is within the tropical cirrus region. Because the background cirrus occurrence frequencies (Figure 5) for those sites outside of the cirrus prevailing regions are not high, more strict cloud screenings in the AERONET observations at these sites are recommended. Statistics were also calculated for four boreal seasons separately but sample sizes are rather limited. Similar to the AERONET-MPLNET comparison, strong seasonal and regional variability were also found for the distributions of SP values over these sites, which tend to be higher during the local thin cirrus prevailing seasons. Statistics also indicate that sample size issues can affect SP values significantly. For example, if we increase the sample size requirement to 40 (equivalent to about two years of CALIPSO and AERONET matched-up data) instead of 20, only 6 sites would have passed the threshold and all of them would have SP values less than 15%, which is closer to the AERONET-MPLNET evaluation results from the 'TW10 existence' testing.

The SP values from the majority of sites in the AERONET-MPLNET and the AERONET-CALIPSO match ups are comparable in the order of magnitude. For example, 60% of the sites have SP values of 4-10% in the 'TW10 existence' testing shown in Table 3, and about half the sites with less than 10% in Figure 5 (note that all sites have SP values less than 15% if the sample size requirement is set to 40). However the discrepancy between AERONET-MPLNET (Tables 3-4 and Figure 3) and AERONET-CALIPSO (Figure 5) was also observed. Possible explanations are the following: 1) The AERONET-MPLNET and AERONET-CALISPO match ups are based on different spatial-temporal domains. The former and latter are related more to time/distance constraints, respectively; 2) MPL and CALIPSO observe cirrus occurrence frequency differently, while the MPL usually has lower values than CALIPSO during cirrus peak seasons, as explained in Section 3.2 (Table 1); and 3) The SP values are highly sensitive to the selection of cirrus detection criteria (see Table 2-4). The tighter the cirrus detection requirements are the less cirrus cases were identified.

3.5 AERONET-MPLNET-CALIPSO 3-Way Matchup

To extend investigations in susceptibility percentage discrepancies between AERONET-MPLNET and AERONET-CALIPSO beyond the match ups of MPLNET-CALIPSO ((Section 3.2), AERONET-MPLNET (Section 3.3), and AERONET-CALIPSO (Section 3.4), it is intriguing to see whether we can identify sufficient samples for a 3-way AERONET-MPLNET-CALIPSO match up. Such data matching is only valid for daytime because AERONET aerosol data are only measured during daytime. A two-step match up procedure was adopted: 1) match up MPLNET-CALIPSO as described in Section 3.2, and identify the MPLNET data collection times that are closest to the CALIPSO overpass; 2) match up AERONET aerosol data around the MPLNET data collection time identified in Step 1. Two different temporal limitations were tested for comparison: 1) any AERONET aerosol AOT 440 nm measurements within 0.5 hour of MPLNET cirrus cases matched up with CALIPSO overpass were considered ‘cirrus susceptible’; 2) any AERONET aerosol measurements within 1 hour of MPLNET cirrus cases matched up with CALIPSO overpass were considered ‘cirrus susceptible’. Unfortunately very few ‘cirrus susceptible’ cases were found from the 3-way comparison for the 9 sites. For the GSFC site, 27 AERONET-MPLNET-CALIPSO matchup cases were identified, where both MPL and CALIPSO agreed on four cirrus cases. Of the four cases, one AERONET matchup was identified as ‘cirrus susceptible’ using the ‘TW30 overall persistence’ testing for the 1-hour time allowance, and none were identified for the 0.5-hour time allowance. It is noted that the numbers are not statistically significant due to the insufficient sample sizes. However, the study successfully demonstrates the 3-way match up approach, which will prove to be more valuable as longer CALIPSO datasets become available and there are more MPLNET-AERONET collocated sites. Collective information resulting from a 3-way data yields improved constraints for cirrus susceptibility testing because it provides two independent verification channels for concurrent cirrus detection.

3.6. AERONET versus MODIS

One of the important objectives of this study is to investigate the feasibility of using satellite derived cloud screening parameters for cloud screening of AERONET aerosol retrievals around the satellite overpass time. Therefore, it is essential to explore the susceptibility of AERONET retrievals to cirrus contamination at AERONET sites during the MODIS overpass times. . Because RR1.38/0.66 is indicative of thin cirrus (Roskovensky and Liou, 2003; Huang et al., 2011), AERONET AOT and Fine Mode Fraction (FMF) measurements were collocated with the MODIS-derived RR1.38/0.66 over select AERONET sites. The 15 AERONET sites were chosen according to their L2.0 AOT data availability and their representativeness on a global map: 4 of them have 5+ year data records and the other 11 have 7+ year data records. Further spatial and temporal constraints for the collocations are: 1) Spatially, considering the 1 km resolution of MODIS L1B data, the closest RR1.38/0.66 value are retrieved within 1 km distance from each AERONET site; 2) temporally, the closest AERONET data points are collected within a ±30 minute time window centered at the MODIS overpass time.

Figure 6 shows overall susceptibility levels of AERONET AOT and FMF data at the 15 sites. For both AOT and FMF, there are 13 (93%) sites having the SP value less than 10%, a comparable SP level to the previous comparisons in AERONET vs. CALIPSO, indicating the effectiveness of current AERONET cloud screening schemes.

Because cirrus cloud particle sizes are larger than aerosols, potential cirrus contamination can be reflected in the changes of the aerosol's particle size distribution; and this phenomenon should become more significant over aerosol emission regions where fine aerosol particles (such as smoke) usually prevail. In order to see the changes of AE and FMF transitioning from cirrus-free to cirrus-contaminated cases, we selected three representative AERONET sites having the longest L2.0 AOT data record over three smoke predominant regions during their peak smoke seasons respectively: Alta_Floresta in Amazon during SON, 2004-2009; Mukdahan in Southeast Asia during MAM, 2004-2009; Mongu in Southern Africa during JJA, 2003-2010. The changes in the PDF of AE and FMF in response to high RR1.38/0.66 at these three sites are shown in Figure 7. Because there were no MPLNET data available at these sites, the collocated MODIS reflectance ratio RR1.38/0.66 was used to distinguish cirrus-contaminated cases from cirrus-free cases. A threshold value of RR1.38/0.66 = 0.1 was used for cirrus cloud identification. Systematic PDF shifting in AE and FMF were observed for all three sites. In comparison to cirrus-free cases, AE and FMF in cirrus-contaminated cases tend to have smaller values, indicating more frequent presence of large particles as a result of possible cirrus contamination. Kosmogorov-Smirnov tests, which are usually used for testing the significance level of differences between two data distributions, indicate that the data distributions of AE and FMF in cirrus-free and cirrus-contaminated cases, as shown in Figures 7, are significantly different at a confidence level of 95%. These evidences are consistent with the theoretical prediction that thin cirrus contamination in the aerosol retrieval would lead to larger retrieved particle sizes, more evidence of potential thin cirrus contamination in AERONET aerosol retrievals.

Such tests of collocating AERONET AOT (or FMF) with the MODIS RR1.38/0.66 cirrus detection parameterization suggests feasible operational routines that can be used to crosscheck aerosol and cirrus retrievals from AERONET and operational satellites.. This becomes more important for satellite product calibration/validation field campaigns where in-situ measurements are closely examined along with collocated satellite observations in near real-time to verify the atmospheric environment and to validate satellite retrievals.

4. Summary and discussions

Concurrent aerosol and cirrus observations from ground measurements and satellites were used to evaluate the susceptibility of ground aerosol retrievals to thin cirrus contamination. We first compared MPLNET and CALIPSO in terms of their cirrus detection capabilities. Their agreement rate is about 71-88% for both day and night match up cases. For the cirrus occurrence frequency, both agreed on the cirrus peak seasons at four selective sites; however, MPLNET detected relatively lower cirrus frequency than CALIPSO during the cirrus peak seasons.

To quantify the susceptibility of the AERONET aerosol products to cirrus contamination, the following pairs of datasets were matched up: 1) AERONET versus MPLNET, 2) AERONET versus CALIPSO, and 3) AERONET versus MODIS. In the AERONET-MPLNET match up, challenges come from the different viewing geometries of the two instruments and difficult cirrus observations at high altitude when the lower atmosphere significantly attenuates lidar signals. For a ‘SZA<20º and TW30 overall cirrus persistence’ testing, all susceptibility percentages at 10 collocated AERONET and

MPLNET sites are less than 5%, and 40% of the sites are less than 1%; for the 'SZA<20º and TW10 existence' testing, 6 out of 10 sites (60%) have SP values within 4-10%, and the other 4 (40%) within 1-3%. The SP values are sensitive to different cirrus detection criteria, such as cirrus persistence test settings, time window selections, and solar zenith angle constraints. An empirical approach for cirrus optical depth calculation based on MPLNET NRB profiles was established and successfully implemented for selective cases to roughly estimate the relative contribution of thin cirrus contamination to AOT retrievals.

Despite various challenges in collocating AERONET with CALIPSO, such as insufficient sampling and distance between CALIPSO daytime tracks and AERONET sites, about half of the 18 AERONET-CALIPSO collocated sites also have a susceptibility percentage less than 10%, a similar order of magnitude to the AERONET-MPLNET match up of data. A promising 3-Way AERONET-MPLNET-CALIPSO match up scheme was established during this study. As CALIPSO lifespan extends and the number of the AERONET-MPLNET supersites increases, the 3-Way comparison will become more valuable when sufficient matchup samples are available. AERONET aerosol retrievals were also paired up with MODIS cirrus parameters, such as RR1.38/0.66, to test the ground-satellite match up techniques in terms of using satellite derived cirrus detection to evaluate cirrus contamination in ground aerosol retrievals. The AERONET-MODIS showed 93% sites having the SP value less than 10%, a comparable SP level to the AERONET-CALIPSO match up. For three smoke dominant regions during their biomass burning seasons, cirrus-free cases and cirrus-contaminated cases were discriminated from each other using the MODIS cirrus parameter, Smaller AERONET Ångström exponents and Fine Mode Fractions were also found in their probability data distributions for 'cirrus-contaminated' cases than in the 'cirrus-free' cases, another indication that thin cirrus potentially contaminates the AERONET aerosol retrievals.

Statistical results from this study demonstrated the effectiveness of the current cloud screening schemes in the AERONET retrieval although residual cirrus contaminated cases may still exist. It is also noteworthy that the susceptibility evaluation is highly dependent on both season and region. Moreover, influential factors, such as viewing geometry differences between sunphotometers and micro-pulse lidars when AERONET and MPLNET are compared, and the sample size threshold values when AERONET and CALIPSO data are compared, can significantly impact the susceptibility percentage. From a cirrus contamination perspective, this study improves our understanding of data uncertainties of ground aerosol products. Similar evaluations on satellite aerosol retrievals are underway. Further improvement of ground aerosol product quality is valuable for calibration and validation of satellite aerosol retrievals, and also very important for any consequential aerosol-related climate research.

Acknowledgement

This work is supported by grant from the NASA EOS Program, managed by Hal Maring. Authors thank Drs. David Giles, Bo-cai Gao, Steve Ou, Larry R. Belcher and Zhien Wang for their constructive comments on the use of in-situ and satellite data, analysis methodology and cirrus climatology. Aqua MODIS L1B data were obtained from NASA L1 and Atmosphere Archive and Distribution System (LAADS). CALIPSO data were obtained from the NASA Langley Research Center Atmospheric Science Data Center. The NASA Micro-Pulse Lidar Network is funded by the NASA Earth Observing System and Radiation Sciences Program.

References

Andreae. M. O., 1991: Biomass Burning: Its History, Use, and Distribution and Its Impact on Environmental Quality and Global Change. *Global Biomass Burningg: Atmospheric, Climatic. and Biospheric Implications* (J. S. Levine, editor), The MIT Press, Cambridge. Mass. pp.3-21.

Berkoff, T., Ji, Q., Kleidman, R., Stewart, S., Welton, E. J., Li, Z., Holben, B., 2008: Ground-based Lidar Measurements During the CALIPSO and Twilight Zone (CATZ) Campaign, *American Geophysical Union, Spring Meeting 2008*, abstract #A33D-14.

Breon, F-M, D. Tanre, S. Generso, 2002: Aerosol effect on cloud droplet size monitored from satellite. *Science*, **295**, 834-838.

Eguchi, K., Uno, I., Yumimoto, K., Takemura, T., Shimizu, A., Sugimoto, N., and Liu, Z., 2009: Trans-pacific dust transport: integrated analysis of NASA/CALIPSO and a global aerosol transport model, *Atmos. Chem. Phys.,* **9**, 3137-3145, doi:10.5194/acp-9-3137-2009.

Gao, B. C., and Y. Kaufman, 1995: Selection of the 1.375 μm MODIS channel for remote sensing of cirrus clouds and stratospheric aerosols from space. *J. Atmos. Sci.,* **52**, 4231–4237.

Gao, B. C., and Y. Kaufman, D. Tanre, and R.-R. Li, 2002a: Distinguishing tropospheric aerosols from thin cirrus clouds for improved aerosol retrievals using the ratio of 1.38μm and 1.24-μm channels. *Geophys. Res. Lett.,* **29**, 1890, doi:10.1029/2002GL015475.

Gao, B. C., Ping Yang; Wei Han; Rong-Rong Li; Wiscombe, W.J., 2002b: An algorithm using visible and 1.38-μm channels to retrieve cirrus cloud reflectances from aircraft and satellite data," *IEEE Trans. Geosci. Remote Sens.*, **40**, 1659-1668, 2002b

Holben, B. N., T. F. Eck, I. Slutsker, D. Tanré, J. P. Buis, A. Setzer, E. Vermote, J. A. Reagan, Y. J. Kaufman, T. Nakajima, F. Lavenu, I. Jankowiak, and A. Smirnov, 1998: AERONET-A federated instrument network and data archive for aerosol characterization. *Remote Sens. Environ.*, **66**, 1-16.

Hsu, N.C., S.-C. Tsay, M.D.King and J. R. Herman (2004). Aerosol properties over bright-reflecting source regions. IEEE T. Geosci. Remote, 42(3), 557-569;

Hsu, N.C., S.-C. Tsay, M.D.King and J. R. Herman (2006). Deep Blue retrieval of asian aerosol properties during ACE-Asia. IEEE T. Geosci. Remote, 44(11), 3180-3195;

Huang, J., N. C. Hsu, S. Tsay, M. Jeong, B. N. Holben, T. A. Berkoff, and E. J. Welton (2011), Susceptibility of aerosol optical thickness retrievals to thin cirrus contamination during the BASE-ASIA campaign, *J. Geophys. Res.*, 116, D08214, doi:10.1029/2010JD014910.

Huang, J. Zhang, C., Prospero, J. M., Aerosol-Induced Large-Scale Variability in Precipitation over the Tropical Atlantic, *Journal of Climate*, 22, 4970-4988, DOI: 10.1175/2009JCLI2531.1, 2009

Kaufman, Y. J., L. A. Remer, D. Tanre, R. R. Li, R. Kleidman, S. Mattoo, R. Levy, T. Eck, B. N. Holben, C. Ichoku, J. Martins, and I. Koren, 2005: A critical examination of the residual cloud contamination and diurnal sampling effects on MODIS estimates of aerosol over ocean. *IEEE Trans. Geosci. Remote Sens.*, **43** (12), 2886-2897.

Kaufman, Y. J., G. P. Gobbi, and I. Koren, 2006: Aerosol climatology using a tunable spectral variability cloud screening of AERONET data. *Geophy. Res. Lett.* **33**, L07817, doi: 10.1029/2005GL025478.

Levine, J. S., D. R. Cahoon, Jr., J. A. Costulis, R. H. Couch, R. E. Davis, P. A. Garn, A. Jalink, Jr., J. A. McAdoo, D. M. Robinson, W. A. Roettker, W. A. Sasamoto, R. T. Sherrill, and K. D. Smith, 1989: FireSat and the Global Monitoring of Biomass Burning. National Research Council.

Liu, Zhaoyan, and Coauthors, 2009: The CALIPSO Lidar Cloud and Aerosol Discrimination: Version 2 Algorithm and Initial Assessment of Performance. *J. Atmos. Oceanic Technol.*, **26**, 1198–1213.

Massie, S. T., J. Gille, C. Craig, R. Khosravi, J. Barnett, W. Read, and D. Winker, 2010: HIRDLS and CALIPSO observations of tropical cirrus, *J. Geophys. Res.*, ***115***, D00H11, doi:10.1029/2009JD012100.

Menon, S., J. Hansen, L. Nazarenko, and Y. Luo, 2002: Climate effects of black carbon aerosols in China and India. *Science,* **297**, 2250-2253.

Myhre, G, F. Stordal, M. Johnsrud, D. J. Diner, I. V. Geogdzhayev, J. M. Haywood, B. N. Holben, T. Holzer-Popp, A. Ignatov, R. A. Kahn, Y. J. Kaufman, N. Loeb, J. V. Martonchik, M. I. Mishchenko, N. R. Nalli, L. A. Remer, M. Schroedter-Homscheidt, D. Tanré, O. Torres, and M. Wang, 2005: Intercomparison of satellite retrieved aerosol optical depth over ocean during the period September 1997 to December 2000, Atmos. Chem. Phys., 5, 1697-1719.

Remer, Tanre, Kaufman, Levy, & Mattoo, 2009: Algorithm for Remote Sensing of Tropospheric Aerosol from MODIS for Collection 005: Revision 2 Products: 04_L2, ATML2, 08_D3, 08_E3, 08_M3

Remer, L. A., Y. J. Kaufman, D. Tanré, S. Mattoo, D. A. Chu, J. V. Martins, R-R. Li, C. Ichoku, R. C. Levy, R. G. Kleidman, T. F. Eck, E. Vermote, & B. N. Holben, 2005: The MODIS Aerosol Algorithm, Products and Validation. Journal of the Atmospheric Sciences, Special Section. Vol 62, 947-973.

Roskovensky, J. K., and K. N. Liou ,T. J. Garrett, and D. Baumgardner, 2004: Simultaneous retrieval of aerosol and thin cirrus optical depths using MODIS airborne simulator data during CRYTAL-FACE and CLAMS, *Geophys. Res. Lett.,* **31**, L18110, doi:10.1029/2004GL020457

Roskovensky, J. K., and K. N. Liou (2003), Detection of thin cirrus from 1.38 mm/0.65 mm reflectance ratio combined with 8.6 – 11 mm brightness temperature difference, *Geophys. Res. Lett.,* **30**(19), 1985, doi:10.1029/ 2003GL018135

Sassen, K., M. K. Griffin, and G. C. Dodd, (1989), Optical scattering and microphysical properties of subvisual cirrus clouds and climatic implications, *J Appl Meteorol*, **28**, pp. 91- 98.

Sassen, K., Z. Wang, and D. Liu (2008), Global distribution of cirrus clouds from CloudSat/Cloud-Aerosol Lidar and Infrared Pathfinder Satellite Observations (CALIPSO) measurements, *J. Geophys. Res.,* **113**, D00A12, doi:10.1029/2008JD009972.

Schaap, M., Apituley, A., Timmermans, R. M. A., Koelemeijer, R. B. A., and de Leeuw, G., 2009: Exploring the relation between aerosol optical depth and PM2.5 at Cabauw, the Netherlands*, Atmos. Chem. Phys.,* **9**, 909-925, doi:10.5194/acp-9-909-2009.

Smirnov, A., B.N. Holben, T.F. Eck, O. Dubovik, and I. Slutsker, 2000: Cloud-screening and quality control algorithms for the AERONET database, *Remote Sens. Environ.*, **73**, 337-349.

Takemura, T., T. Nozawa, S. Emori, T. Y. Nakajima, and T. Nakajima, 2005: Simulation of climate response to aerosol direct and indirect effects with aerosol transport-radiation model, J. Geophys. Res., 110, D02202, doi:10.1029/2004JD005029.

Tao, W.-K., X. Li, A. Khain, T. Matsui, S. Lang, and J. Simpson, 2007: Role of atmospheric aerosol concentration on deep convective precipitation: Cloud-resolving model simulations, J. Geophys. Res., 112, D24S18, doi:10.1029/2007JD008728.

Vaughan, M. A., et al., 2005: CALIOP algorithm theoretical basis document, part 2: Feature detection and layer properties algorithms, Rep PC-SCI-202.02, NASA Langley Research Center, Hampton, VA 23681, 87pp. [available online at http://www-calipso.larc.nasa.gov/resources/project_documentation.php]

Vaughan, M. A., and Coauthors, 2009: Fully Automated Detection of Cloud and Aerosol Layers in the CALIPSO Lidar Measurements. *J. Atmos. Oceanic Technol.*, **26**, 2034–2050.

Welton, E. J., J. R. Campbell, J. D. Spinhirne, and V. S. Scott, Global monitoring of clouds and aerosols using a network of micro-pulse lidar systems, in Lidar Remote Sensing for Industry and Environmental Monitoring, U. N. Singh, T. Itabe, N. Sugimoto, (eds.), *Proc. SPIE,* **4153**, 151-158, 2001.

Table and Figure List

Table 1. A comparison between MPLNET and CALIPSO on the seasonality of daytime thin cirrus occurrence frequency (%). The values for MPLNET are the percentage of cirrus cases over the total MPLNET measurements during +/-30 minutes around the CALIPSO daytime overpass time. The values for CALIPSO are thin cirrus occurrence frequency observed from all CALIPSO track overpasses at each site within the 1×1 degree grid centered at each site. The highest and lowest seasons are highlighted for each site.

Table 2. Statistics on the MPLNET-CALIPSO match up over the 9 AERONET-MPLNET collocated sites during daytime (the left outlined data block) and nighttime (the right outlined data block)

Table 3. Susceptibility percentage (SP, %) of AERONET Level 2.0 AOT retrievals to thin cirrus contamination, and its sensitivity to cirrus existence and persistence criteria settings, time window (TW) and solar zenith angle (SZA), in the left, middle and right thick line outlined data blocks respectively. Samples are from all seasons.

Table 4. Seasonality of susceptibility percentage (SP, %) of AERONET Level 2.0 AOT retrievals to thin cirrus contamination, and its sensitivity to cirrus existence and persistence criteria settings. Two types of cirrus persistence criteria settings (TW10 existence and TW30 overall persistence) are shown in the left and right thick line outlined data blocks respectively.

Figure 1. (a) Daytime thin cirrus occurrence frequency (%) and (b) Daytime thin cirrus daytime average height (km) in each 5°×5° grid as calculated from CALIPSO VFM (December 2006 – November 2007).

Figure 2. An example cirrus occurrence case over COVE AERONET and MPLNET site on June 7, 2007: (a) MPL L1.0 normalized relative backscatter (NRB) higher than 0.35; (b) MPL statistical cirrus flag (SCF); (c) MPL statistical cirrus persistence flag (CPF); and (d) AERONET AOT and Ångström exponent measurements, and solar zenith angle (SZA) (note the SZA for the data measurement around 9am was 41°, which did not pass the SZA<20º test and is therefore off the chart).

Figure 3. Susceptibility percentage (SP, %) of AERONET L2.0 AOT retrievals to thin cirrus contamination as tested against the MPLNET statistical cirrus flag. Refer to Sections 2.2 and 3.3.1 for more details of match up criteria.

Figure 4. Cirrus optical depth estimation for cirrus cases over GSFC on June 7, 2007: (a) NRB profile from 12 to 20 UTC (local 7am to 5pm). The two matchup cases are highlighted by vertical lines; (b) cirrus optical depth calculation results for the case of 16:12UTC; and (c) cirrus optical depth calculation results for the case of 16:22UTC.

Figure 5. Susceptibility percentage (SP, %) tests of AERONET L2.0 AOT retrievals against the CALIPSO vertical feature mask. Refer to Section 3.4 for more details of the one-to-one match up criteria.

Figure 6. Susceptibility percentage map of AERONET aerosol retrievals against MODIS derived RR1.38/0.66 over 15 AERONET sites. The four eastern most sites were selected with 5+ years of L2.0 AOT data record; and all the remaining sites were selected with 7+ years of L2.0 AOT data records available. SP values (%) in red are for AOT and yellow for FMF.

Figure 7. PDF of AE and FMF for cirrus and non-cirrus cases over three representative AERONET sites for smoke prevailing regions during peak smoke seasons (from left to right: Alta_Floresta in Amazon during SON, 2004-2009; Mukdahan in Southeast Asia during MAM, 2004-2009; Mongu in Southern Africa during JJA, 2003-2010). Top panels (a-c) are for AE and bottom panels (d-f) are for FMF. RR1.38/0.66>0.1 was used for thin cirrus case identification.

Tables

Table 1. A comparison between MPLNET and CALIPSO on the seasonality of daytime thin cirrus occurrence frequency (%). The values for MPLNET are the percentage of cirrus cases over the total MPLNET measurements during +/-30 minutes around the CALIPSO daytime overpass time. The values for CALIPSO are thin cirrus occurrence frequency observed from all CALIPSO track overpasses at each site within the 1×1 degree grid centered at each site. The highest and lowest seasons are highlighted for each site.

Site	UTC	MPLNET (%)					CALIPSO (%)				
		MAM	JJA	SON	DJF	4-Season	MAM	JJA	SON	DJF	4-Season
GSFC	18.0-19.0	**11.37**	**15.65**	15.24	14.14	14.10	17.88	**20.30**	**12.40**	13.02	18.56
COVE	17.9-18.9	11.94	**13.95**	**10.35**	13.24	12.62	15.21	**24.33**	**11.90**	15.24	16.56
Trinidad_Head	20.7-21.7	**12.27**	**3.38**	7.27	11.34	8.13	**32.65**	**9.09**	10.51	17.08	16.12
NCU_Taiwan	5.0-6.0	5.33	**9.59**	5.31	**0.76**	5.36	9.38	**17.66**	5.27	**3.48**	8.66

Table 2. Statistics on the MPLNET-CALIPSO match up over the 9 AERONET-MPLNET collocated sites during daytime (the left outlined data block) and nighttime (the right outlined data block)

Site	Cases	Day	MPL	VFM	Both	Agreement % (Day)	Night	MPL	VFM	Both	Agreement % (Night)	**Agreement % (Day&Night)**
GSFC	Cirrus	90km	5 (1)	5	4 (1)		40km	10 (3)	14	5 (3)		
	Non-Cirrus		22	22	21			51	47	42		
	Total Cases		27	27	25	92.59%		61	61	47	77.05%	**81.82%**
COVE	Cirrus	50km	24 (0)	13	8 (0)		20km	15 (3)	23	9 (3)		
	Non-Cirrus		48	59	43			54	46	40		
	Total Cases		72	72	51	70.83%		69	69	49	71.01%	**70.92%**
NCU	Cirrus	30km	2 (0)	7	1 (0)		70km	5 (1)	7	2 (1)		
	Non-Cirrus		60	55	54			54	52	49		
	Total Cases		62	62	55	88.71%		59	59	51	86.44%	**87.60%**
Trinidad_head	Cirrus	30km	2 (0)	2	1 (0)		40km	8 (3)	7	4 (2)		
	Non-Cirrus		20	20	19			25	26	22		
	Total Cases		22	22	20	90.91%		33	33	26	78.79%	**83.63%**
Gosan_SNU	Cirrus	10km	5 (0)	9	2 (0)		No samples.					
	Non-Cirrus		43	39	36							
	Total Cases		48	48	38	79.17%						**79.17%**
Monterey	Cirrus	30km	4 (0)	7	1 (0)		20km	4 (2)	8	4 (2)		
	Non-Cirrus		36	33	30			38	34	34		
	Total Cases		40	40	31	77.50%		42	42	38	90.48%	**84.14%**
Barbados	Cirrus	80km	0 (0)	0	0 (0)		50km	12 (3)	21	10 (3)		
	Non-Cirrus		1	1	1			35	26	24		
	Total Cases		1	1	1	100%		47	47	34	72.34%	**72.92%**
Singapore	Cirrus	80km	2 (0)	4	1 (0)		No samples.					
	Non-Cirrus		10	8	7							
	Total Cases		12	12	8	66.67%						**66.67%**
Kanpur	Cirrus	35km	4 (2)	3	1 (1)		70km	2 (0)	3	2 (0)		
	Non-Cirrus		21	22	19			5	4	4		
	Total Cases		25	25	20	80%		7	7	6	85.71%	**81.25%**

Notes: In the ‘MPL’ column, the numbers outside brackets are from the ‘TW10 existence’ tests, and the numbers inside brackets are from the ‘TW30 strong persistence’ tests. Similarly, in the ‘Both’ row, the numbers are the corresponding MPL cases that agreed with the CALIPSO VFM cirrus testing. In the last column, ‘agreement %’ is the percentage of MPL and CALIPSO agreed cases over the total matchup cases. The distance (km) in the ‘Day’ and ‘Night’ columns are allowance thresholds of the distance between the site and the CALIPSO overpass tracks.

Table 3. Susceptibility percentage (SP, %) of AERONET Level 2.0 AOT retrievals to thin cirrus contamination, and its sensitivity to cirrus existence and persistence criteria settings, time window (TW) and solar zenith angle (SZA), in the left, middle and right thick line outlined data blocks respectively. Samples are from all seasons.

Site Name	MPLNET Coverage	Sensitivity of SP (%) to cirrus existence and persistence criteria settings (Sample Size N: cirrus/total)				Sensitivity of SP (%) to time window (Sample Size N: cirrus/total)			Sensitivity of SP (%) to SZA (Sample Size N: cirrus/total)	
		SZA<20º TW10 Existence	**SZA<20º TW30 Existence**	**SZA<20º TW30 Overall persistence**	**SZA<20º TW30 Strong persistence**	SZA<20º TW15 **Strong persistence**	SZA<20º TW30 **Strong persistence**	SZA<20º TW60 **Strong persistence**	SZA<20º TW30 **Strong persistence**	All SZA TW30 **Strong persistence**
GSFC	2001.11-2010.06	7.74 (45/581)	3.61 (21/581)	3.44 (20/581)	1.55 (9/581)	3.10 (18/581)	1.55 (9/581)	1.20 (7/581)	1.55 (9/581)	3.29 (1265/38437)
COVE	2004.05-2010.09	4.44 (11/248)	2.82 (7/248)	2.42 (7/248)	2.82 (7/248)	4.03 (10/248)	2.82 (7/248)	2.82 (7/248)	2.82 (7/248)	2.21 (186/8409)
Trinidad_Head	2005.05-2010.09	1.14 (2/175)	0 (0/175)	0 (0/175)	0 (0/175)	0 (0/175)	0 (0/175)	0 (0/175)	0 (0/175)	2.10 (223/10612)
NCU_Taiwan	2005.01-2009.10	4.00 (6/150)	0.67 (1/150)	0.67 (1/150)	0.67 (1/150)	1.33 (2/150)	0.67 (1/150)	0.67 (1/150)	0.67 (1/150)	4.10 (139/3394)
Gosan_SNU	2007.04-2010.02	4.76 (5/105)	0.95 (1/105)	0.95 (1/105)	0.95 (1/105)	1.90 (2/105)	0.95 (1/105)	0 (0/105)	0.95 (1/105)	0.68 (11/1620)
Monterey	2003.04-2003.10 2004.01-2004.04 2007.03-2009.04	2.44 (19/780)	1.41 (11/780)	1.41 (11/780)	0.26 (2/780)	1.41 (11/780)	0.26 (2/780)	0 (0/780)	0.26 (2/780)	2.80 (537/19152)
Ragged_Point	2008.06-2011.09	1.95 (16/819)	0.49 (4/819)	0.49 (4/819)	0.49 (4/819)	0.98 (8/819)	0.49 (4/819)	0.24 (2/819)	0.49 (4/819)	4.17 (344/8242)
Singapore	2009.09-2011.09	6.35 (24/378)	2.65 (10/378)	2.65 (10/378)	0.79 (3/378)	2.91 (11/378)	0.79 (3/378)	0 (0/378)	0.79 (3/378)	4.85 (239/4923)
Kanpur	2009.05-2010.09	2.36 (9/381)	1.31 (5/381)	1.31 (5/381)	1.31 (5/381)	1.60 (6/375)	1.31 (5/381)	1.60 (6/375)	1.31 (5/381)	2.74 (127/4634)
Pimai	2006.02-2006.05	8.33 (14/168)	3.57 (6/168)	3.57 (6/168)	2.38 (4/168)	5.52 (9/163)	2.38 (4/168)	0 (0/163)	2.38 (4/168)	8.65 (148/1711)
Skukuza	1999.08-1999.09 2000.08-2000.09	--	--	--	--	--	--	--	--	0.26 (3/1176)
Mongu	2000.08-2000.09	0 (0/16)	0 (0/16)	0 (0/16)	0 (0/16)	0 (0/16)	0 (0/16)	0 (0/16)	0 (0/16)	0.72 (7/978)
XiangHe	2005.02-2005.05	--	--	--	--	--	--	--	--	1.74 (21/1207)

(Note: the numbers inside brackets are the sample size of 'cirrus cases' over the total sample size of 'cirrus and non-cirrus cases', as the calculations of SP values. The SP values with the 'TW30 overall persistence' tests were plotted in Figure 3).

Table 4. Seasonality of susceptibility percentage (SP, %) of AERONET Level 2.0 AOT retrievals to thin cirrus contamination, and its sensitivity to cirrus existence and persistence criteria settings. Two types of cirrus persistence criteria settings (TW10 existence and TW30 overall persistence) are shown in the left and right thick line outlined data blocks respectively.

Site Name	MAM SP%	JJA SP%	SON SP%	DJF SP%	All Seasons, SP (%)	MAM SP%	JJA SP%	SON SP%	DJF SP%	All Seasons, SP (%)
	SZA<20º TW10 Existence	**SZA<20º TW10 Existence**	**SZA<20º TW10 Existence**	**SZA<20º TW10 Existence**	**SZA<20º TW10 Existence**	**SZA<20º TW30 Overall Persistence**	**SZA<20º TW30 Overall Persistence**	**SZA<20º TW30 Overall Persistence**	**SZA<20º TW30 Overall Persistence**	**SZA<20º TW30 Overall Persistence**
GSFC	7.09 (9/127)	7.93 (36/454)	--	--	**7.74 (45/581)**	0.79 (1/127)	4.19 (19/454)	--	--	**3.44 (20/581)**
COVE	2.54 (3/118)	6.15 (8/130)	--	--	**4.44 (11/248)**	0.85 (1/117)	4.10 (5/122)	--	--	**2.42 (7/248)**
Trinidad_Head	0 (0/2)	1.16 (2/173)	--	--	**1.14 (2/175)**	0 (0/2)	0 (0/173)	--	--	**0 (0/175)**
NCU_Taiwan	11.1 (4/36)	2.04 (2/98)	(0/16)		**4.00 (6/150)**	2.78 (1/36)	0 (0/98)	0 (0/16)	--	**0.67 (1/150)**
Gosan_SNU	0 (0/59)	10.87 (5/46)	--	--	**4.76 (5/105)**	0 (0/59)	2.17 (1/46)	--	--	**0.95 (1/105)**
Monterey	5.88 (11/187)	1.35 (8/593)			**2.44 (19/780)**	4.28 (8/187)	0.51 (3/593)	--	--	**1.41 (11/780)**
Ragged_Point	1.32 (4/303)	1.11 (4/360)	5.13 (8/156)	--	**1.95 (16/819)**	0.33 (1/303)	0.28 (1/360)	1.28 (2/156)	--	**0.49 (4/819)**
Singapore	5.56 (3/54)	9.33 (7/75)	6.81 (13/191)	1.72 (1/58)	**6.35 (24/378)**	1.85 (1/54)	2.67 (2/75)	3.66 (7/191)	0 (0/58)	**2.65 (10/378)**
Kanpur	1.43 (2/140)	2.90 (7/241)	--	--	**2.36 (9/381)**	0.71 (1/140)	1.66 (4/241)	--	--	**1.31 (5/381)**
Pimai	8.33 (14/168)	--	--	--	**8.33 (14/168)**	3.57 (6/168)	--	--	--	**3.57 (6/168)**
Skukuza	--	--	--	--	--	--	--	--	--	--
Mongu	--	--	0 (0/16)	--	**0** (0/16)	--	--	0 (0/16)	--	**0 (0/16)**
XiangHe	--	--	--	--	--	--	--	--	--	--

Figure

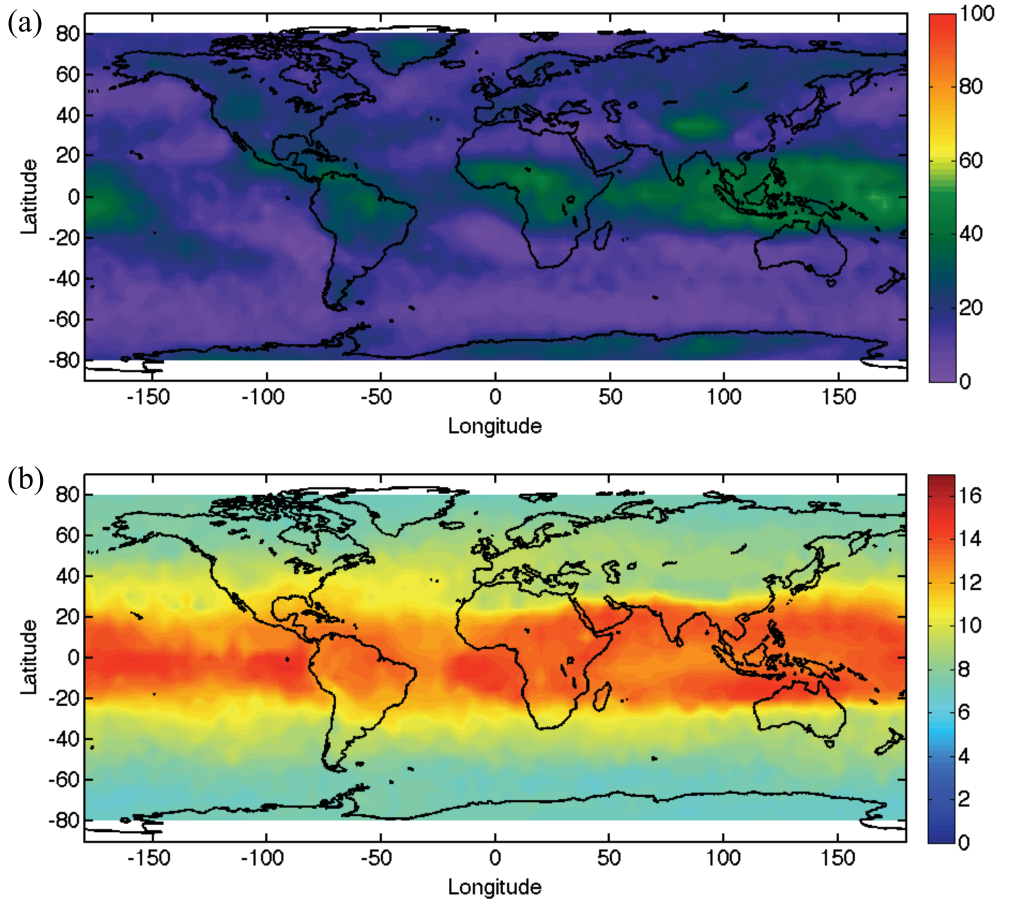

Figure 1. (a) Daytime thin cirrus occurrence frequency (%) and (b) Daytime thin cirrus daytime average height (km) in each 5°×5° grid as calculated from CALIPSO VFM (December 2006 – November 2007).

(a)

(b)

(c)

(d)

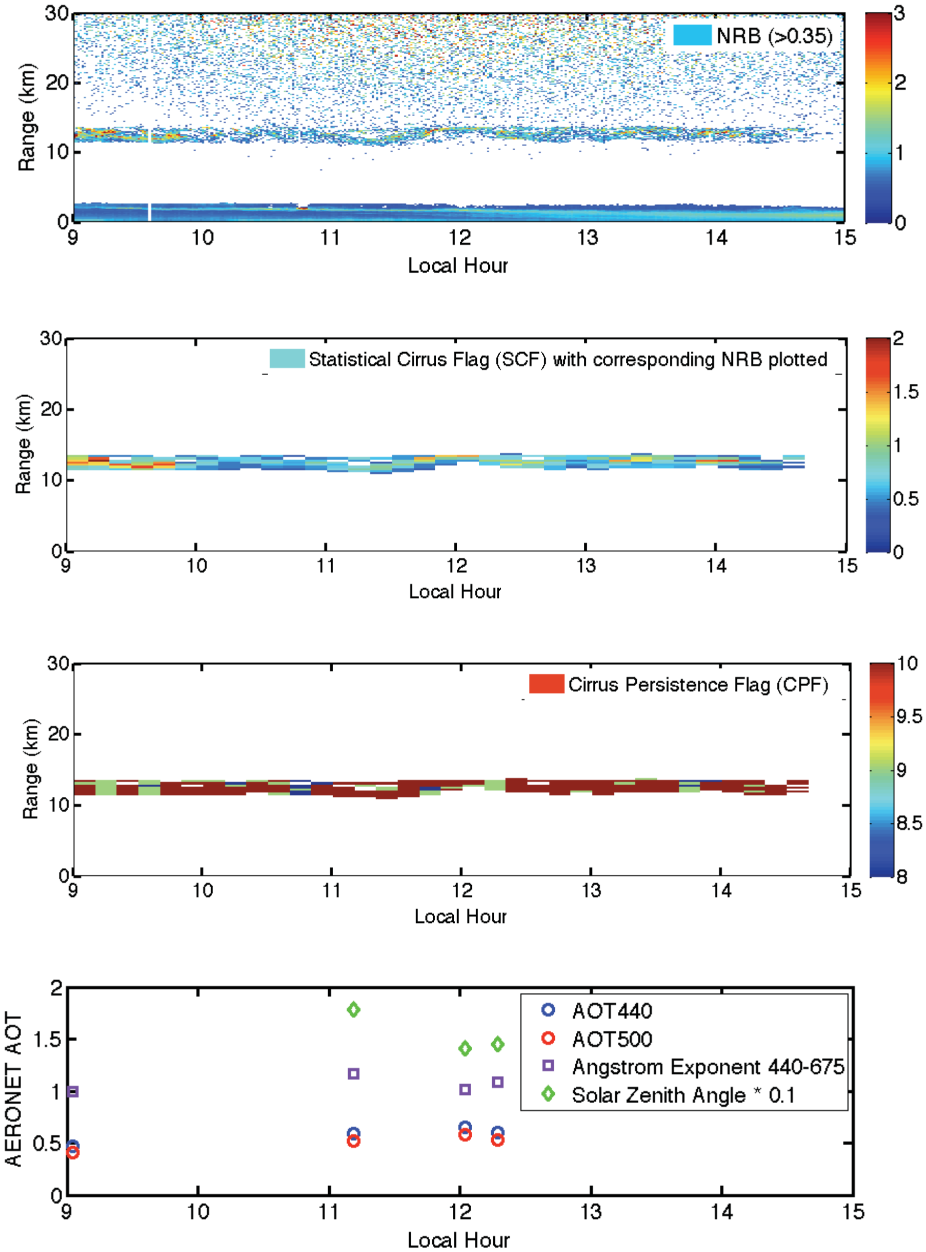

Figure 2. An example cirrus occurrence case over COVE AERONET and MPLNET site on June 7, 2007: (a) MPL L1.0 normalized relative backscatter (NRB) higher than 0.35; (b) MPL statistical cirrus flag (SCF); (c) MPL statistical cirrus persistence flag (CPF); and (d) AERONET AOT and Ångström exponent measurements, and solar zenith angle (SZA) (note the SZA for the data measurement around 9am was 41°, which did not pass the SZA<20º test and is therefore off the chart).

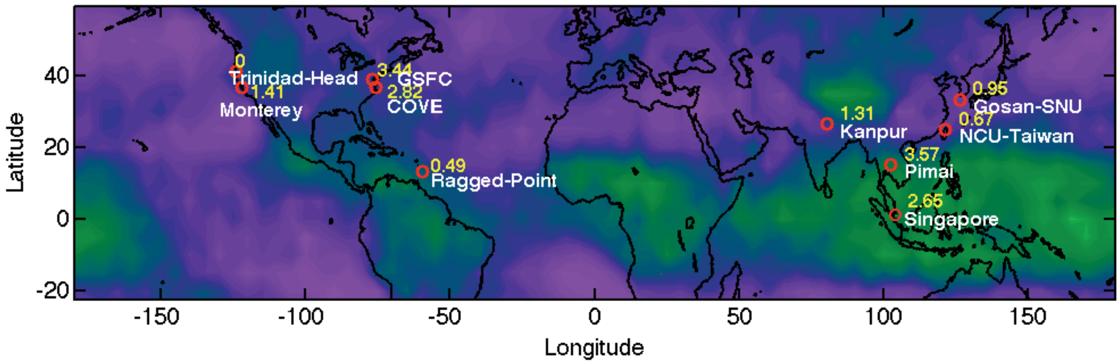

Figure 3. Susceptibility percentage (SP, %) of AERONET L2.0 AOT retrievals to thin cirrus contamination as tested against the MPLNET statistical cirrus flag. Refer to Sections 2.2 and 3.3.1 for more details of match up criteria.

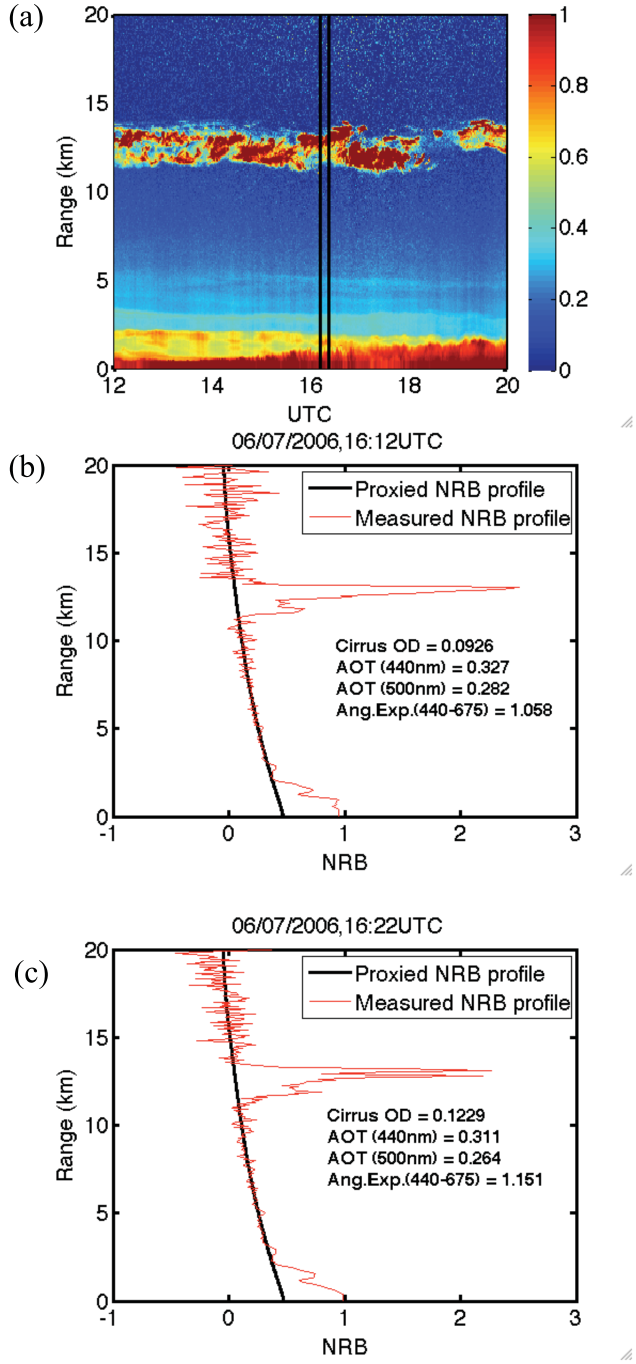

Figure 4. Cirrus optical depth estimation for cirrus cases over GSFC on June 7, 2007: (a) NRB profile from 12 to 20 UTC (local 7am to 5pm). The two matchup cases are highlighted by vertical lines; (b) cirrus optical depth calculation results for the case of 16:12UTC; and (c) cirrus optical depth calculation results for the case of 16:22UTC.

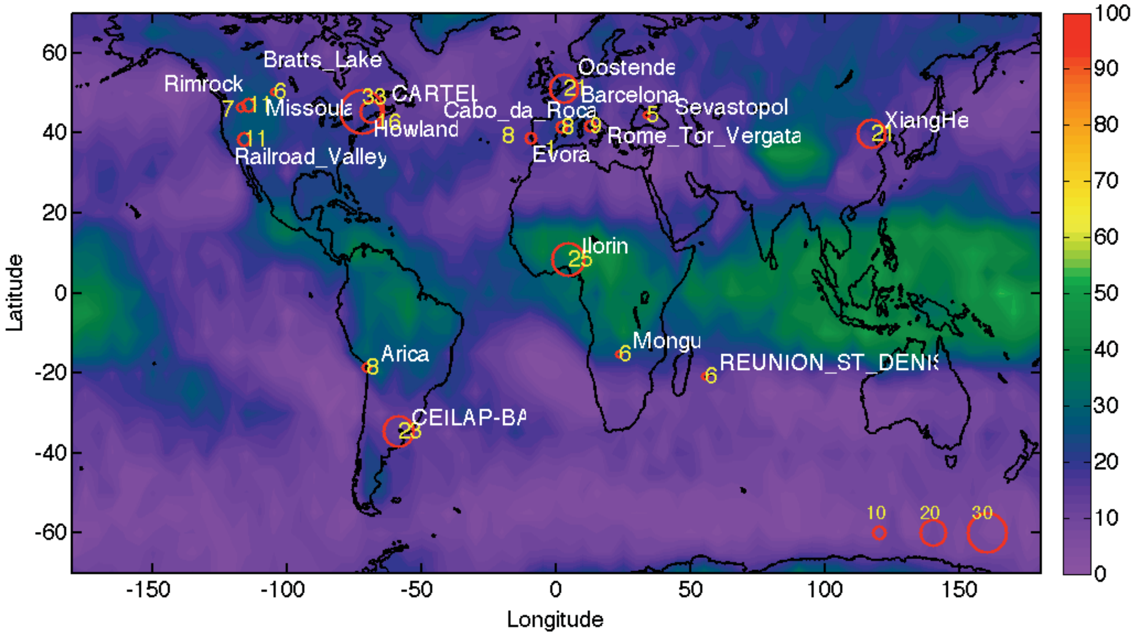

Figure 5. Susceptibility percentage (SP, %) of AERONET L2.0 AOT retrievals as tested against the CALIPSO vertical feature mask. Refer to Section 3.4 for more details of the one-to-one match up criteria.

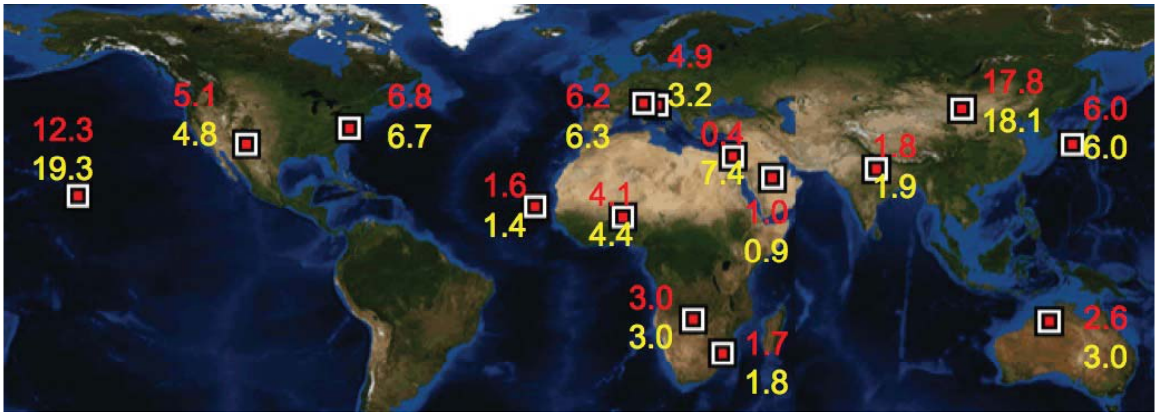

Figure 6. Susceptibility percentage map of AERONET aerosol retrievals against MODIS derived RR1.38/0.66 over 15 AERONET sites. The four eastern most sites were selected with 5+ years of L2.0 AOT data record; and all the remaining sites were selected with 7+ years of L2.0 AOT data records available. SP values (%) in red are for AOT and yellow for FMF.

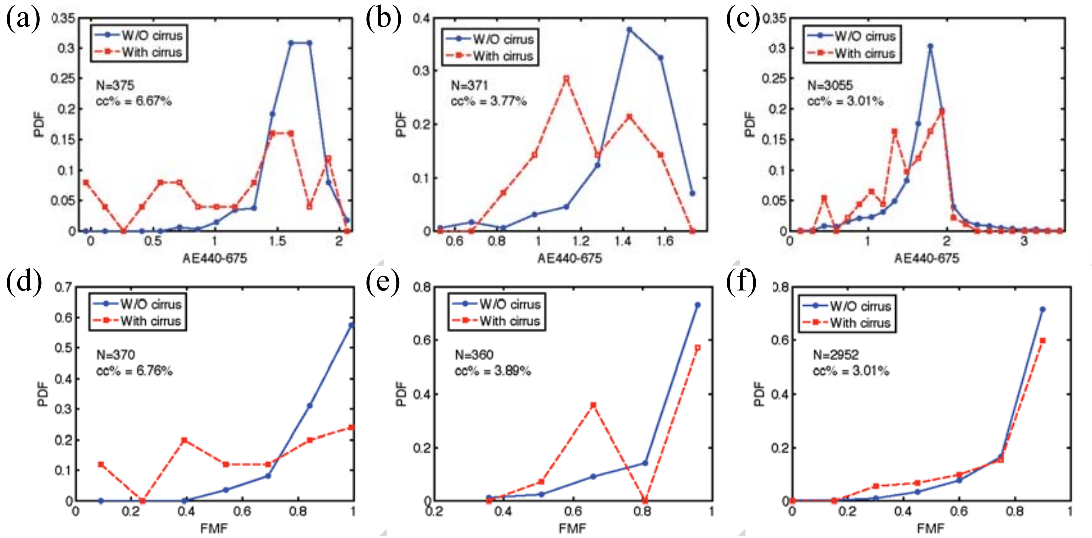

Figure 7. PDF of AE and FMF for cirrus and non-cirrus cases over three representative AERONET sites for smoke prevailing regions during peak smoke seasons (from left to right: Alta_Floresta in Amazon during SON, 2004-2009; Mukdahan in Southeast Asia during MAM, 2004-2009; Mongu in Southern Africa during JJA, 2003-2010). Top panels (a-c) are for AE and bottom panels (d-f) are for FMF. RR1.38/0.66>0.1 was used for thin cirrus case identification.

Acronyms/Abbreviation LIST

Acronyms/Abbreviation	Full Name
AE	Ångström exponent
AERONET	Aerosol Robotic Network
AOT	Aerosol Optical Thickness
BASE-ASIA	Biomass-burning Aerosols in South East-Asia: Smoke Impact Assessment field campaign
CALIOP	Cloud-Aerosol LIdar with Orthogonal Polarization
CALIPSO	Cloud-Aerosol Lidar and Infrared Pathfinder Satellite Observations
CPF	Cirrus Persistence Flag
DJF	December-January-February
FMF	Fine Mode Fraction
JJA	June-July-August
MAM	March-April-May
MODIS	Moderate Resolution Imaging Spectroradiometer
MPL	Micro-Pulse Lidar
MPLNET	Micro-Pulse Lidar Network
NCEP	National Centers for Environmental Prediction
NRB	Normalized Relative Backscatter
RR	Reflectance Ratio
SCF	Statistical Cirrus Flag
SON	September-October-November
SP	Susceptibility Percentage
SZA	Solar Zenith Angle
TW	Time Window
VFM	Vertical Feature Mask